



Synthesis, Spectral Characterization and Biological Activity of Dithiocarbamate-based Ligand and its Metal Complexes

Farah Z. Al-Obeidi¹, Aeed S. Al-Fahdawi², Mohamad J. Al-Jeboori^{3*}

¹Department of Chemistry, College of Education for Pure Science, University of Anbar, Iraq.

²Department of Chemistry, College of Education for Women, University of Anbar, Iraq.

³Department of Chemistry, College of Education for Pure Science (Ibn Al-Haitham), University of Baghdad, Adhamiyah, Baghdad, Iraq.

Abstract

This work is based on the synthesis, structural characterization and biological activity of some dithiocarbamate-based complexes. The free dithiocarbamate ligand was prepared via several synthetic routes including the formation of Schiff-base. The reaction of 2,6-diaminopyridine with benzaldehyde resulted in the formation of Schiff-base which reduced to the corresponding diamine by methanolic NaBH₄. The reaction of diamine with CS₂ in a methanolic solution of KOH resulted in the preparation of the free dithiocarbamate ligand. Macrocyclic complexes were formed from the reaction of the appropriate metal chloride with the ligand in an ethanolic medium. The suggested geometries around metal centres were determined using a range of physicochemical and spectroscopic techniques. The analytical and spectroscopic data revealed the formation of four and six coordinate complexes. Complexes of the general formula [M(L)]₂ (where M= Fe(II), Co(II) and Zn(II) indicated metal centres adopt tetrahedral geometries. Complexes with the general formula [M(L)(H₂O)₂]₂ (where M= Mn(II), Ni(II), Cu(II) indicated octahedral structures around metal centres. Biological activity of the ligand and its complexes against four strains of bacteria (*Escherichia coli* (*E. coli*), *Pseudomonas aeruginosa*, *Bacillus cereus* and *Staphylococcus aureus*) and antifungal activity against two types of pathogenic fungi, *Aspergillus niger* and *Aspergillus parasiticus* are tested.

Keywords: Dithiocarbamate ligand; Transition metal complexes; Spectral characterization; Biological activity.

Introduction

Dithiocarbamates (DTCs) species are interesting organic molecules that have chelating ability towards transition metal ions and representative elements [1, 2].

Their importance encouraged researchers to explore intensively the chemistry, synthetic routes and mechanisms of reaction of sulphur-containing compounds by finding new ways to introduce sulphur atom into compounds at lower cost and greater yield [8]. DTCs and their complexes display important applications in biological system [3], medicinal chemistry [4], in environmental chemistry, materials and industrial application [5].

Further, dithiocarbamate (dtc) species are promising candidates that have shown anticancer, antibacterial and antifungal activities [6]. These species have also shown

a role in medicine. An anticancer example is the formation of triazole- dithiocarbamate hybrids which are designed to be selectively LSD1 in-activators. They are attacking gastric cancer cell growth, by invasion and migration [7].

Further, dtcs have shown application in analytical chemistry. The Si-dtcs compounds have shown sensitivity in the determination of Pb(II), Cd(II), Cu(II) and Hg(II) from aqueous solutions [8]. Laintz et al, used selectively lithium bis (trifluoroethyl) dithiocarbamate for separation of arsenic(III) and antimony(III) from natural water [9].

Furthermore, ammonium pyrrolidine dithiocarbamate reagent was used as a simple, rapid, and environmentally friendly precursor for the extraction of cadmium in fruit and vegetables, compared with other

micro-extraction techniques [10]. More, dtc-compounds have been used in biomedical application. Recently, researchers are exploring the possibility of replacing benzimidazole (dte), and chalcone- dtcs, instead of cis-platinum [11].

Experimental

Materials

2,6-Diaminopyridine, benzaldehyde, methanol, potassium hydroxide, carbon disulphide and dimethyl sulfoxide (DMSO) were purchased from Sigma-Aldrich and used without further purification. Solvents were distilled prior to use.

Physical Measurements

Elemental analyses (C, H, N and S) for compounds were carried using Euro Vector, model EA 3000.

Melting points of compounds were conducted using an Electro-Thermal Stuart melting point apparatus. Fourier transform infrared spectra (FTIR) were recorded on a Shimadzu (FT-IR)-8400S spectrophotometer in the range ($4000 - 200 \text{ cm}^{-1}$). Spectra were obtained as KBr and CsI discs.

The electronic spectra for ligands and their complexes were measured using a Shimadzu UV-Visible 160A Spectrophotometer, in DMSO solutions, with (10^{-3} - 10^{-5} M) concentration. ^1H NMR spectra were recorded on a Bruker 500MHz SWISS TS AG. Metal content of complexes were determined using a Shimadzu (A.A) 620G atomic absorption spectrophotometer.

The conductivity measurements of the complexes were recorder at (25°C) for (10^{-3} mole L^{-1}) solution of the samples in DMSO using a Jenway conductivity meter model 4070. Magnetic moments were determined at room temperature with a Sherwood Scientific Apparatus.

Synthesis

Preparation of Schiff-base N, N-(pyridine-2,6-diyl) bis (1-phenyl methanimine)

Benzaldehyde (0.5g, 4.6mmol) was added with stirring to a mixture of 2,6-diaminopyridine (0.25g, 2.30mmol) dissolved in methanol (25mL), and then 5 drops of acetic acid was added to the solution.

The mixture was allowed to reflux for 3 h, and then filtered off. Upon removing solvent under reduced pressure, a yellow solid was formed which collected by filtration and washed with ether (10mL). Yield: 0.46g (76.62%).

Preparation of secondary amine N, N-dibenzyl-N-N-dimethylpyridine-2,6-diamine

To a solution of N, N-(pyridine-2,6-diyl) bis (1-phenyl methanimine) (0.25g, 0.87mmol) in 30mL of dichloromethane/methanol (2:1), was added in small portions an excess of NaBH_4 (0.65g, 1.75mmol).

The mixture was allowed stirring overnight. H_2O (200mL) was added and the product was extracted into CH_2Cl_2 (4 x 50mL) and then washed again with H_2O (200mL) and dried over K_2CO_3 . Filtration followed by solvent removal under vacuum gave the product as yellow oil. Yield: 0.37g (61.7 %).

Synthesis of Potassium Pyridine-2,6-diylbis (benzylcarbamo-dithioate) (L)

To a mixture of (0.25g, 0.87mmol) of secondary amine (1) dissolved in (25mL) methanol, was added a solution of KOH (0.12g, 2.19mmol) dissolved in (2mL) methanol. The mixture was allowed to stir in an icy bath for 30 min, and then a solution of CS_2 (0.13g, 1.75mL) was added and the mixture kept stirring for 18 h.

After that the potassium dithiocarbamate salt that obtained was collected by filtration, washed with MeOH (5mL) and dried under vacuum. Yield: 0.58g (68.83 %).

General Synthesis of Macrocylic-based Complexes

An ethanolic solution (25 mL) of 1 mmol of the metal chloride salt was added with stirring into an ethanolic solution of the ligand (1 mmol) in ethanol (25 mL). The reaction mixture was stirred at room temperature for 24 h.

A solid was formed, which was collected by filtration, washed by methanol (5 mL) and then dried under vacuum. Elemental analysis data, colours, and yields for the complexes are given in (Table 1).

Biological Activity

The biological activity of the ligand and

selected complexes, $[\text{Co}(\text{L})]_2$, $[\text{Cu}(\text{L})(\text{H}_2\text{O})_2]_2$ and $[\text{Zn}(\text{L})]_2$, was studied on four different types of bacteria and two types of fungi.

Determination of Bacteriological Activity

Tested solutions were performed on the ligand and some of its complexes using DMSO solution. The concentrations were (50, 100, 150, 200) mg / mL.

The minimum and maximum limits of these concentrations (50 and 200) mg/mL were selected for biological activity. Bioactivities were investigated using agar-well diffusion method [12].

The wells were dug in the media with the help of a sterile metallic borer with centres at least 24 mm. Recommended concentration (50 and 200) mg/mL in DMSO was introduced in the respective wells.

The plates were incubated immediately at 37°C for 24 hours. Activity was determined by measuring the diameter of zones showing complete inhibition (mm).

In order to clarify the role of DMSO in the biological screening, separate studies were carried out with the solutions alone of DMSO and they showed no activity against any bacterial strains.

All these complexes were found to be potentially active against these bacterial strains, except for the strain of *Bacillus cereus* bacteria, only $[\text{Co}(\text{L})]_2$ showed an effective against it.

Determination of Antifungal Activity

The antifungal activity of ligand and some of its complexes was studied against two fungal cultures, *Aspergillus niger* and *Aspergillus parasiticus*. Potato dextrose agar (PDA) [13] was used in this study.

To prepare the PDA, 1 L of distilled water was mixed with 36 g of PDA powder. The media was sterilized in autoclave at 121°C for 1 h before use. Pour the nutritious medium into Petri dishes and the medium consists of (17 mL PDA + 3 mL of the prepared complex) with the same concentrations as above.

These concentrations were inoculated with fungus and at the rate of two holes of isolation for each concentration, and then the spore suspensions were transferred to petri plates using the perforated.

It incubated at 25 ° C for 24 hours, and then read the results from 1-5 days to a week in a row. [14].

Results and Discussion

The reaction of 2, 6-diaminopyridine with benzaldehyde in a mole ratio 1:2 gave the required Schiff-base, which reduced to the corresponding diamine using NaBH_4 .

The reaction of diamine precursor with CS_2 in a mole ratio 1:2 resulted in the isolation of the dithiocarbamate ligand in a good yield, see Scheme 1.

The formation of dithiocarbamate-based macrocyclic complexes were achieved from the reaction of the ligand with the desired metal ion in a 1:1 mole ratio.

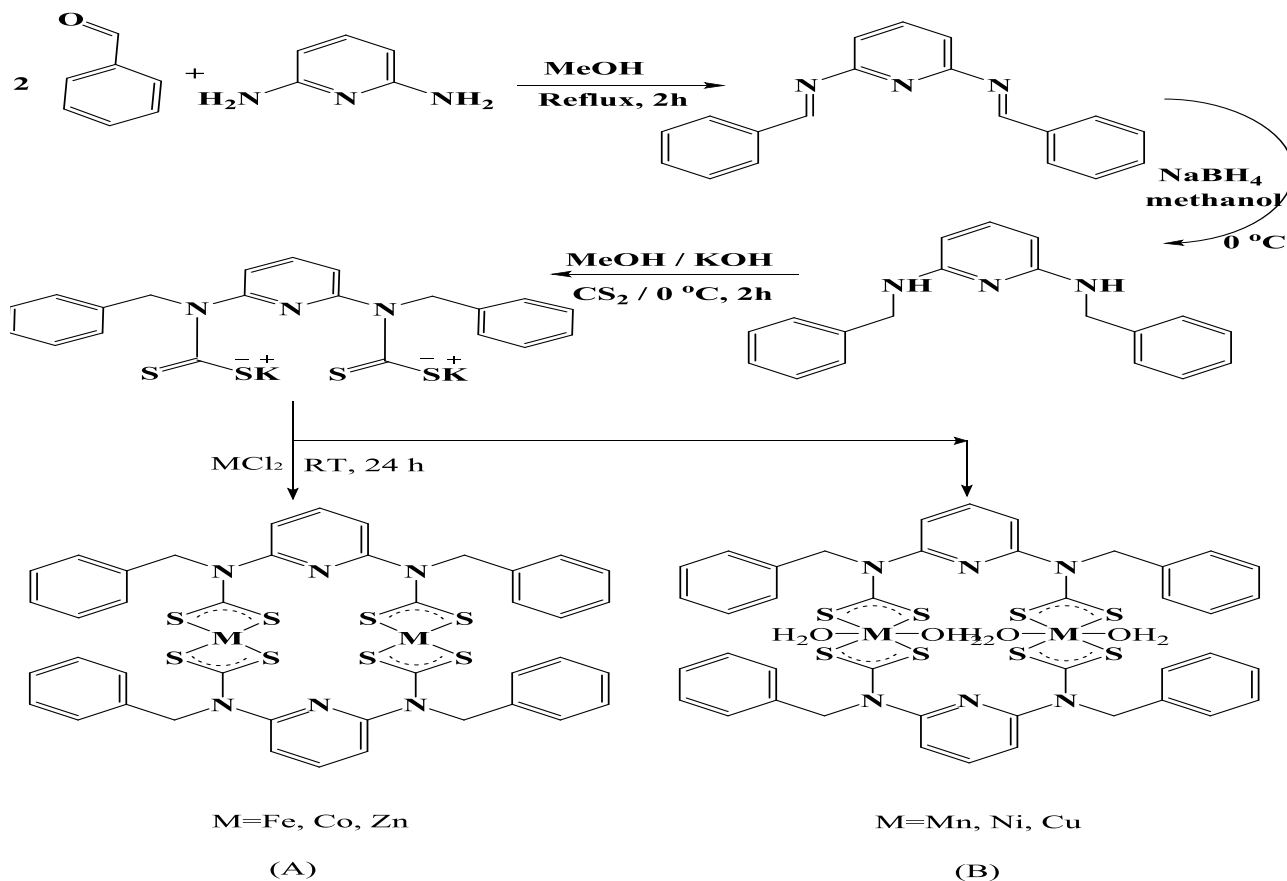
In this method, the metal ion played the key role in the self-assembly of the desired dinuclear macrocyclic complexes.

Physico-chemical analysis revealed the isolation of four and six coordinate complexes of the general formula $[\text{M}(\text{L})]_2$ (where M= Fe(II), Co(II), Zn(II) and $[\text{M}(\text{L})(\text{H}_2\text{O})_2]_2$ (where M= Mn(II), Ni(II), Cu(II), respectively (see Scheme 1).

The complexes are air stable solid, completely soluble in DMSO and not in common organic solvents.

The new ligand and its dinuclear macrocyclic complexes were characterised by elemental analysis, melting point, conductance, FTIR, electronic spectra, mass spectroscopy, ^1H -NMR and magnetic measurement. The analytical data (Table 1) agree well with the suggested formulae.

The molar conductance of the complexes in DMSO solutions is indicative of their non-electrolytic nature.



Scheme 1: Synthetic route of ligand and its complexes; (A) $[\text{M}(\text{L})]_2$; where $\text{M}=\text{Fe}^{\text{II}}, \text{Co}^{\text{II}}, \text{Zn}^{\text{II}}$, and (B) $[\text{M}(\text{L})(\text{H}_2\text{O})_2]_2$; where $\text{M}=\text{Mn}^{\text{II}}, \text{Ni}^{\text{II}}, \text{Cu}^{\text{II}}$.

FTIR Spectra

The FTIR spectra of L and its complexes are depicted together in Figure (1-A, B, see supporting information). FTIR spectra of L and its complexes exhibited two bands in the region $1604\text{-}1573\text{cm}^{-1}$ that referred to $\nu(\text{C}=\text{N})$ and $\nu(\text{C}=\text{C})$ of the pyridyl ring. The strong band in the range $1480\text{-}1492\text{ cm}^{-1}$ in the spectra of complexes are attributed to the $\nu(\text{N}-\text{CS}_2)$ stretching vibration. This band shows an increase of the carbon-nitrogen double bond character, compared with the free ligand that observed at 1467 cm^{-1} [16]. The $\nu_{\text{as}}(\text{CS}_2)$, which shows bands at 1124 and 999 cm^{-1} in the ligand [17], is shifted and appeared around 1045 and 995 cm^{-1} in the complexes.

The $[\text{Mn}(\text{L})(\text{H}_2\text{O})_2]_2$ and $[\text{Ni}(\text{L})(\text{H}_2\text{O})_2]_2$ complexes exhibited two bands at $489, 327$ and $498, 371.7\text{ cm}^{-1}$, which assigned to $\nu(\text{Mn}-\text{S})$ and $\nu(\text{Ni}-\text{S})$, respectively confirming the anisobidentate chelation mode of the ligand [18]. The assignments of prominent bands of complexes are tabulated in Table (2) see supporting information. L= potassium pyridine-2,6-diylbis (benzylcarbamodithioate)

GC-EI (+) Mass Spectrum of L

The GC-EI (+) mass spectrum of L is depicted in Figure (2). see supporting information. The spectrum reveals successive fragments related to the L structure, with the appropriate isotope distribution pattern. The parent ion peak for L is observed at $m/z = 517.96 (\text{M})^+$ (12 %) for $\text{C}_{21}\text{H}_{17}\text{N}_3\text{S}_4$; requires $=517.58$. Peaks observed at $m/z = 408.07$ (2 %), 362.08 (2.3 %), 289.16 (55 %), 199.11 (100 %) and 109.06 (62%) are assigned to $[\text{C}_{21}\text{H}_{17}\text{N}_3\text{S}_3]^+$, $[\text{C}_{20}\text{H}_{16}\text{N}_3\text{S}_2]^+$, $[\text{C}_{19}\text{H}_{19}\text{N}_3]^+$, $[\text{C}_{12}\text{H}_{13}\text{N}_3]^+$ and $[\text{C}_5\text{H}_7\text{N}_3]^+$, respectively. Scheme 2 (See supporting information) illustrates the fragmentation pattern of L.

Electronic Spectra and Magnetic Susceptibility

The UV-Vis spectral data for $[\text{M}(\text{L})]_2$ (where: $\text{M}=\text{Fe}^{\text{II}}, \text{Co}^{\text{II}}, \text{Zn}^{\text{II}}$) and $[\text{M}(\text{L})(\text{H}_2\text{O})_2]_2$ (where: $\text{M}=\text{Mn}^{\text{II}}, \text{Ni}^{\text{II}}, \text{Cu}^{\text{II}}$) are depicted in Figures (3-9, see supporting information). The spectra show peaks around $265\text{-}367\text{ nm}$ assigned to intra-ligand field in the complexes [25]. Peaks detected around visible region $375\text{-}430\text{ nm}$ were attributed to charge transfer. The electronic spectra of the Fe (II)

complex exhibited peaks at 591nm related to ${}^5E_1(D) \rightarrow {}^5T_2(D)$, and the magnetic moments value of μ_{eff} is 4.12 B.M indicating tetrahedral geometry [19]. The electronic spectra of the Co(II) complexes exhibited peaks around 673 nm assigned to ${}^4T_1g(F) \rightarrow {}^4T_1g(P)$, which could be attributed to the spin allowed d-d transitions in a tetrahedral geometry about Co-atom [20]. This data are in agreement with the magnetic moment value of μ_{eff} at 4.06 B.M, for tetrahedral geometry around Co atom. However, the spectra of the Zn complex exhibited bands around 273, 343 and 426 nm assigned to ligands $\pi \rightarrow \pi^*$, $n \rightarrow \pi^*$ and charge transfer.

These complexes are diamagnetic as expected and normally prefer tetrahedral coordination. The electronic spectra of the Mn(II) complex exhibited peaks at 622 nm related to ${}^6A_{1g} \rightarrow {}^4T_{1g}(G)$, and the magnetic moments value of μ_{eff} is 2.48 B.M indicating octahedral geometry [21]. The electronic spectra of the Ni-complex exhibited peak at 600 nm related to ${}^3T_{2g} \rightarrow {}^3T_{1g}(F)$, indicating octahedral geometry about Ni atom [16]. The magnetic moments value of μ_{eff} at 3.29 B.M as well as the other analytical data is in agreement with octahedral geometry around Ni atom. The Cu-complex showed peak around 611 nm, related to ${}^2B_{1g} \rightarrow {}^2E_g$ confirming an octahedral geometry about metal centre [21].

${}^1\text{H-NMR}$ Spectra

The predicted ${}^1\text{H}$ NMR spectrum of the free ligand was generated using the Chem Draw Professional 15.0 Program [22]. The aim of this was to compare the chemical shifts of different protons with that recorded for Zn-complex, (Figure 10). The predicted ${}^1\text{H}$ NMR spectrum of the free ligand showed peak at $\delta = 5.85$ ppm (2H) referred to ($C_{7,7}\text{-H}$).

Chemical shift at $\delta = 7.04$ ppm assigned to ($C_8\text{-H}$). While, resonances in the aromatic region at $\delta = 7.28$ ppm equivalent to 10 protons assigned to (10H, $C_{1,1}, 2, 2, 3, 3, 4, 4, 5, 5\text{-H}$). Signal at $\delta = 4.83$ ppm. That appeared as a singlet, attributed to ($-\text{CH}_2$; $C_{6,6}\text{-H}$). See supporting information Figure (10). The recorded ${}^1\text{H}$ NMR spectrum for $[\text{Zn}(\text{L}^2)]_2$ displays chemical shift at $\delta = 5.25$ ppm equivalent to four protons assigned to (4H, $C_{7,7}, 17, 17\text{-H}$). The complex indicated signal at $\delta = 6.97$ ppm (2H, t, $J_{\text{HH}} = 7.33$ Hz) assigned to ($C_8, C_{18}\text{-H}$). Chemical shifts collected at $\delta = 7.15\text{-}7.35$ ppm are equivalent to 20 aromatic protons, which assigned to ($C_{1,1}, 2,$

$2, 3, 3, 4, 4, 5, 5, 11, 11, 12, 12, 13, 13, 14, 14, 15, 15\text{-H}$) protons. Signal at $\delta = 5.10$ ppm is related to ($C_{6,6}, 16, 16\text{-H}$), that connected to ($-\text{N-CS}_2$) groups. This signal is shifted downfield, compared with the simulation of free ligand. Signal observed at chemical shift ca. $\delta = 2.50$ ppm is due to dimethyl sulfoxide, see supporting information Figure (11).

Biological Activity

Antibacterial Activity

The free dithiocarbamate ligand and its metal complexes were screened against *Staphylococcus aureus*, *Escherichia coli*, *Pseudomonas aeruginosa* and *Bacillus cereus* to assess their potential as an antimicrobial agent by disc diffusion method. The measured zone of inhibition against the growth of various microorganisms is listed in Table (2), compared with some standard drugs that used in the market, see Tables (3). It is found that the metal complexes have higher antimicrobial activity than the free ligand.

The increased activity of the complexes can be explained on the basis of chelation theory and Overtone's model [23]. According to the chelation theory, the complex formation could help the complex to cross a cell membrane of microorganism. This is due the chelation significantly reduces the polarity of the metal ion and allows partial sharing of the positive metal charge with the donor groups. This can be done by delocalisation of metal charge into the ligand π -system, over the whole of chelate system. This will increase the lipophilic nature of the metal chelate system which prefers its penetration through lipid layer of the cell membranes of microorganism [24].

Antifungal Activity

The free dithiocarbamate ligand and its complexes with Co(II), Cu(II), Zn(II) ions were tested against two types of pathogenic fungi, *Aspergillus niger* and *Aspergillus parasiticus*. The obtained results are tabulated in Table (4). The inhibitory effect of the tested compounds indicated a significant inhibitory activity on *Aspergillus niger* and *Aspergillus parasiticus* at concentration (50-200 mg/ml). The free dithiocarbamate ligand (L) and its complexes exhibited higher activity against *Aspergillus niger* and *Aspergillus parasiticus* compared with some antifungal medication that used in the market, see (Table (5)).

The overall observation indicated that the activity, as antifungal and antibacterial tested compounds pronounced more biological

Table 1: Colours, yields, melting points, (C, H, N, S) analysis, and molar conductance values complexes

Metal ion	Colour	Yield (%)	m.p. °C					S \square M(cm ² mol ⁻¹)	
			M%	C	H	N	S		
Mn ^{II}	Light brown	42.85	Over 340	10.31 (10.34)	47.36 (47.38)	4.35 (4.39)	7.89 (7.90)	24.08 (24.12)	2.6
Fe ^{II}	Light brown	14.28	Over 340	11.23 (11.25)	50.70 (50.75)	3.85 (3.88)	8.45 (8.47)	25.78 (25.82)	3.1
Co ^{II}	Light red	59.52	180-182	11.77 (11.79)	50.39 (50.42)	3.83 (3.86)	8.39 (8.43)	25.62 (25.64)	12.8
Ni ^{II}	Light brown	65.07	280*	10.94 (10.97)	47.03 (47.08)	4.32 (4.37)	7.83 (7.85)	23.91 (23.95)	2.4
Cu ^{II}	Green	67.46	270*	11.74 (11.75)	46.60 (46.66)	4.28 (4.31)	7.76 (7.77)	23.69 (23.72)	17.2
Zn ^{II}	Yellow	31.74	200-203	12.89 (12.93)	49.75 (49.77)	3.78 (3.90)	8.29 (8.32)	25.29 (25.33)	11.7

*=Decomposed

Table 2: The inhibitory effectiveness of a number of compounds studied in the growth of a number of negative and positive bacteria (diameter of the inhibition area measured in millimetres)

Comp	Conc.	<i>Escherichia coli</i>	<i>Pseudomonase aeruginosa</i>	<i>Staphylococcus aureus</i>	<i>Bacillus cereus</i>
L	50	--	--	--	--
	200	27	--	--	--
[Zn(L)] ₂	50	--	23	--	--
	200	--	45	--	--
[Co(L)] ₂	50	30	24	40	--
	200	35	55	50	42
[Cu(L)(H ₂ O) ₂] ₂	50	29	--	--	--
	200	32	30	--	--

(--)= No inhibition zone

Table 3: The inhibitory activity of a number of control factors (antibiotics) in the growth of a number of positive and negative bacteria (diameter inhibition in millimeters)

Comp	Names of Standard drugs	Conc	<i>Escherichia coli</i>	<i>Pseudomonase aeruginosa</i>	<i>Staphylococcus aureus</i>	<i>Bacillus cereus</i>
1	Tetracycline	50	20	36	28	33
		200	34	39	36	38
2	Ampicillin	50	--	26	27	20
		200	--	40	38	40
3	Streptomycin	50	27	21	38	40
		200	36	41	44	45
4	Ciprofloxacin	50	25	25	30	10
		200	25	50	50	30

Table 4: The inhibitory effectiveness of a number of compounds studied in the growth of a number of fungi (diameter of the inhibition area measured in millimetres)

Comp	Conc	<i>Aspergillus niger</i>	<i>Aspergillus parasiticus</i>
		Control = 45 mm	Control = 43 mm
L	50	--	--
	200	--	--
[Zn(L)] ₂	50	4	3
	200	--	--
[Co(L)] ₂	50	--	--
	200	--	--
[Cu(L)(H ₂ O) ₂] ₂	50	11	8
	200	--	--

(--)=No growth of fungi

Table 5: The inhibitory activity of a number of control factors(antibiotics) in the growth of a number of fungi (diameter inhibition in millimeters)

Comp	Names of Standard drugs	Conc	<i>Aspergillus niger</i>	<i>Aspergillus parasiticus</i>
1	Nystatin	50	10	17
		200	5	10
2	Griseofulvin	50	5	26
		200	2.5	10

Conclusion

The synthesis and characterization of dithiocarbamate-based ligand and some of its macrocyclic complexes are described. The

ligand was performed via three steps. This was based on the formation of Schiff base which reduced to the corresponding diamine using NaBH₄. The reaction of diamine with

CS₂ in presence of KOH gave the required ligand, which reacted with metal ions to give a series of complexes. The mode of bonding and overall structures of the complexes were determined through physico-chemical and spectroscopic methods. These results revealed that Fe(II), Co(II) and Zn(II) complexes adopt tetrahedral geometries about the metal centre. While, complexes of Mn(II) Ni(II) and Cu(II) indicated octahedral

structures around metal centre. Biological activity of the complexes was evaluated among the different bacterial strains and fungal strains. Among the pathogens (*Escherichia coli* (*E. coli*), *Pseudomonas aeruginosa*, *Bacillus cereus* and *Staphylococcus aureus*) and fungi, *Aspergillus niger* and *Aspergillus parasiticus*, were highly susceptible to the complexes.

References

- H Nabipour, S Ghammamy, S Ashuri, ZS Aghbolaghi (2010) "Synthesis of a New Dithiocarbamate Compound and Study of Its Biological Properties", *J. Org. Chem.*, 2, 75-80.
- S Kanchi, P Singh, K Betty (2014) "Dithiocarbamates as hazardous remediation agent: A critical review on progress in environmental chemistry for inorganic species studies of 20th century", *Arabian Journal of Chemistry.*, 7, 11-25.
- PJ heard (2005) "Main group dithiocarbamate complexes", *Prog. Inorg. Chem, USA*, 53, 1-69.
- M Altaf, MM ul-Mehboob, K Abdel-Nasser, G Corona, R Larcher, M Ogasawara, N Casagrande, M Celegato, C Borghese, ZH Siddik, D Aldinucci, AA Isab (2017) "New bipyridine gold(III) dithiocarbamate-containing complexes exerted a potent anticancer activity against cisplatin-resistant cancer cells independent of p53 status", *Oncotarget*, 8,1, 490-505.
- N Awang, I Baba, M Yamin, MS Othman, NF Kamaludin (2011) "Synthesis, Characterization and Biological Activities of Organotin (IV) Methylcyclohexyldithiocarbamate Compounds", *American Journal of Applied Sciences.* 8, 4, 310-317.
- SQ Shah, MR Khan (2011) "Radiosynthesis and biological evaluation of the ^{99m}Tc-tricarbonyl moxifloxacin dithiocarbamate complex as a potential *Staphylococcus aureus* infection radiotracer", *Appl. Radiat. Isot.*, 69, 4, 686-690.
- YC Zheng, YC Duan, JL Ma, RM Xu, X Zi, WL Lv, MM Wang, XW Ye, S Zhu, D Mobley, Y Y Zhu, JW Wang, JF Li, ZR Wang, W Zhao, HM Liuet (2014) "Triazole-dithiocarbamate based, selective LSD1 inactivators inhibit gastric cancer cell growth, invasion and migration", *J Med Chem.*, 14, 56, 21.
- L Bai, H Hu, W Fu, J Wan, X Cheng, L Zhugi, L Zyong, Q Chen (2011) "Synthesis of a novel silica-supported dithiocarbamate adsorbent and its properties for the removal of heavy metal ions", *Journal of Hazardous Materials.*, 195, 261- 275.
- KE Laintz, GM Shieh, CM Wai (1992) "Simultaneous Determination of Arsenic and Antimony Species in Environmental Samples using Bis(trifluoroethyl)dithiocarbamate Chelation and Supercritical Fluid Chromatography", *Journal of Chromatographic Science.*, 30, (4): 120-123.
- M Soylak, E Yilmaz (2015) "Determination of Cadmium in Fruit and Vegetables by Ionic Liquid Magnetic Micro extraction and Flame Atomic Absorption Spectrometry", *Analytical Letters.*, 48, (3) 464-476.
- K Bacharaju, SR Jambula, ST Sivan, V Mangab, SJ Design (2012) "Design, synthesis, molecular docking and biological evaluation of new dithiocarbamates substituted benzimidazole and chalcones as possible chemotherapeutic agents", *Bioorganic & Medicinal Chemistry Letters.*, 22, (9): 3274-3277.
- Atta-ur-Rahman, MI Choudhary, WJ Thomsen (2001) *Bioassay Techniques for Drug Development*, Harwood Academic, Amsterdam, The Netherlands.
- C Booth (1971) *The Genus Fusarium*, Commonwealth Mycological Institute 237.
- C Udayasoorian, PC Prabu (2005) "Biodegradation of phenols by ligninolytic Fungus. *Tramets versicolor*", *Journal of Biological Sciences.*, 5, 824-827.
- AG Sykes, G Wilkinson, RD Gillard, JA McCleverty (1987) "Comprehensive Coordination Chemistry", Pergamon Press: Oxford., UK, 229.
- G Faraglia, S Sitran, D Montagner (2005) "Pyrrolidine dithiocarbamates of Pd(II)", *Inorg. Chim. Act a.*, 358, 971-980.
- BFG Johnson, KH Al-Obaidi, JA Mecleverty (1969) "Transition-metal nitrosyl compounds. Part III. (NN-dialkyldithiocarbamate) nitrosyl compounds of molybdenum and tungsten", *J. Am. Chem. Soc. A.*, 19, 1668-1670.
- AS Al-Fahdawi (2014) "Metal Ion Assisted In Bimetallic Complexes Formation Of New Bis-Dithiocarbamate Macrocyclic Compounds", A Thesis for the Degree of Doctor, University of Babylon.
- MJ Al-Jeboori, AJ Abdul-Ghani, AJ Al-Karawi (2009) "Synthesis and spectral studies of new N2S2 and N2O2 Mannich base ligands and their metal complexes", *J. Coord. Chem.*, 62, 2736-2744.
- MJ Al-Jeboori, FA Al-Jebouri, MA R Al-Azzawi (2011) "Metal complexes of a new class of polydentate Mannich bases: Synthesis and spectroscopic characterization", *Inorg. Chim. Acta.*, 379, 1, 163-170.
- S.A A Nami, A Husain, I Ullah (2014) "Self assembled homodinuclear dithiocarbamates" One pot synthesis", *Spectrochimica Acta Part A: Molecular and Biomolecular Spectroscopy.*, 118, 380-388. 160 *CS Chem 3D Ultra Molecular*

Modelling and Analysis, C, www.cambridgesoft.com.

22. RV Singh, R Dwivedi, SC Joshi (2004) Synthetic, magnetic, spectral, antimicrobial and antifertility studies of dioxomolybdenum(VI) unsymmetrical imine complexes having a N/N donor system", *Transition Metal Chemistry.*, 29, 70-74.
23. HL Singh, JB Singh, S Bhanuka (2016) "Synthesis, spectroscopic characterization, biological screening, and theoretical studies of organotin (IV) complexes of semicarbazone and thiosemicarbazones derived from (2-hydroxyphenyl)(pyrrolidin-1-yl)methanone", *Res Chem. Inter med.* 42, 997.
24. EI Yousif, RM Ahmed, HA Hasan, AS Al-Fahdawi, MJ Al-Jeboori (2017) "Metal Complexes of Heterocyclic Hydrazone Schiff-Bases: Preparation, Spectral Characterization and Biological Study", *Iranian Journal of Science and Technology* 41, 1, 103-109.

SUPPORTING INFORMATION

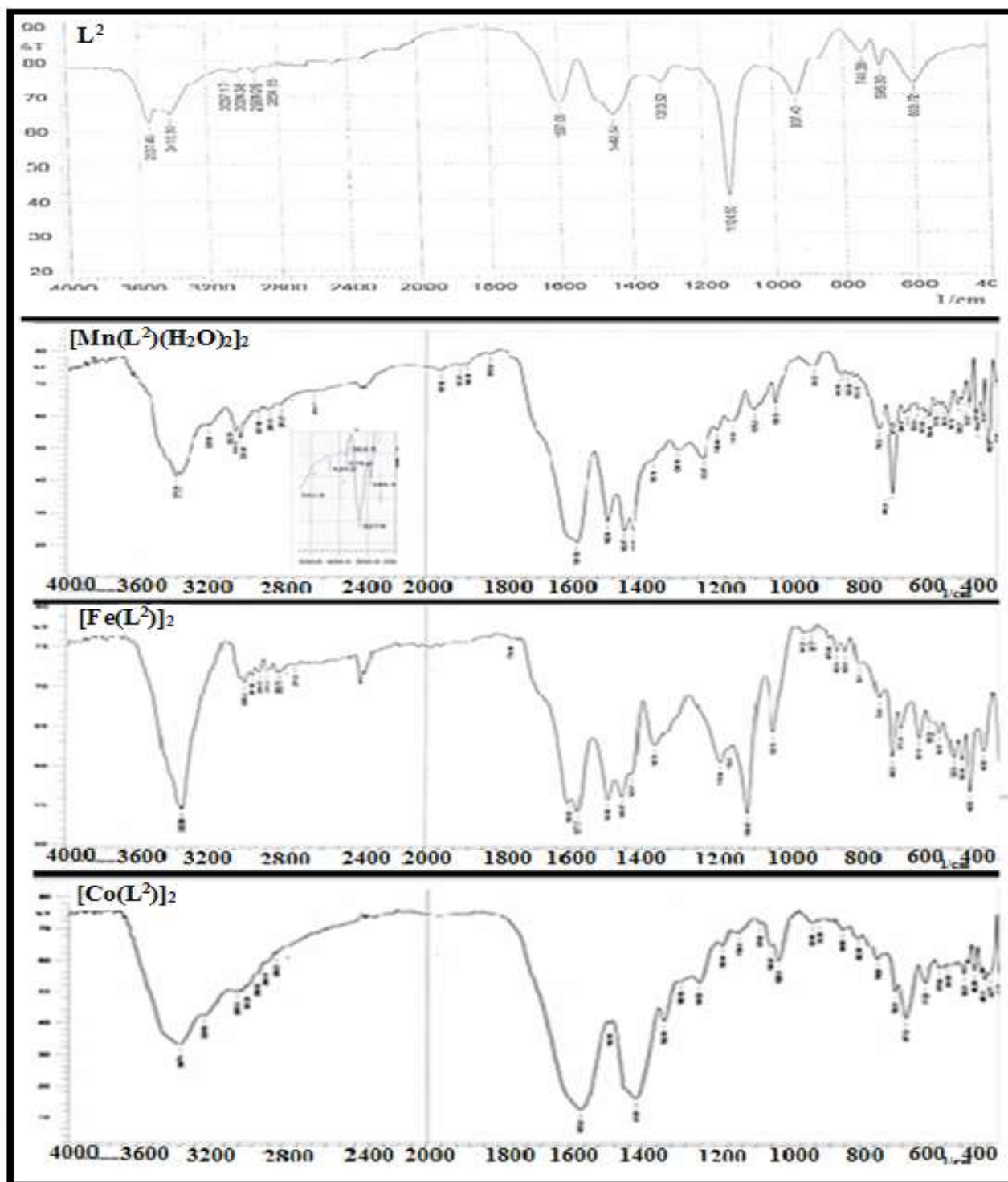


Fig 1-A: FTIR Spectra of L and its complexes with Mn^{II}, Fe^{II} and Co^{II} metal ions

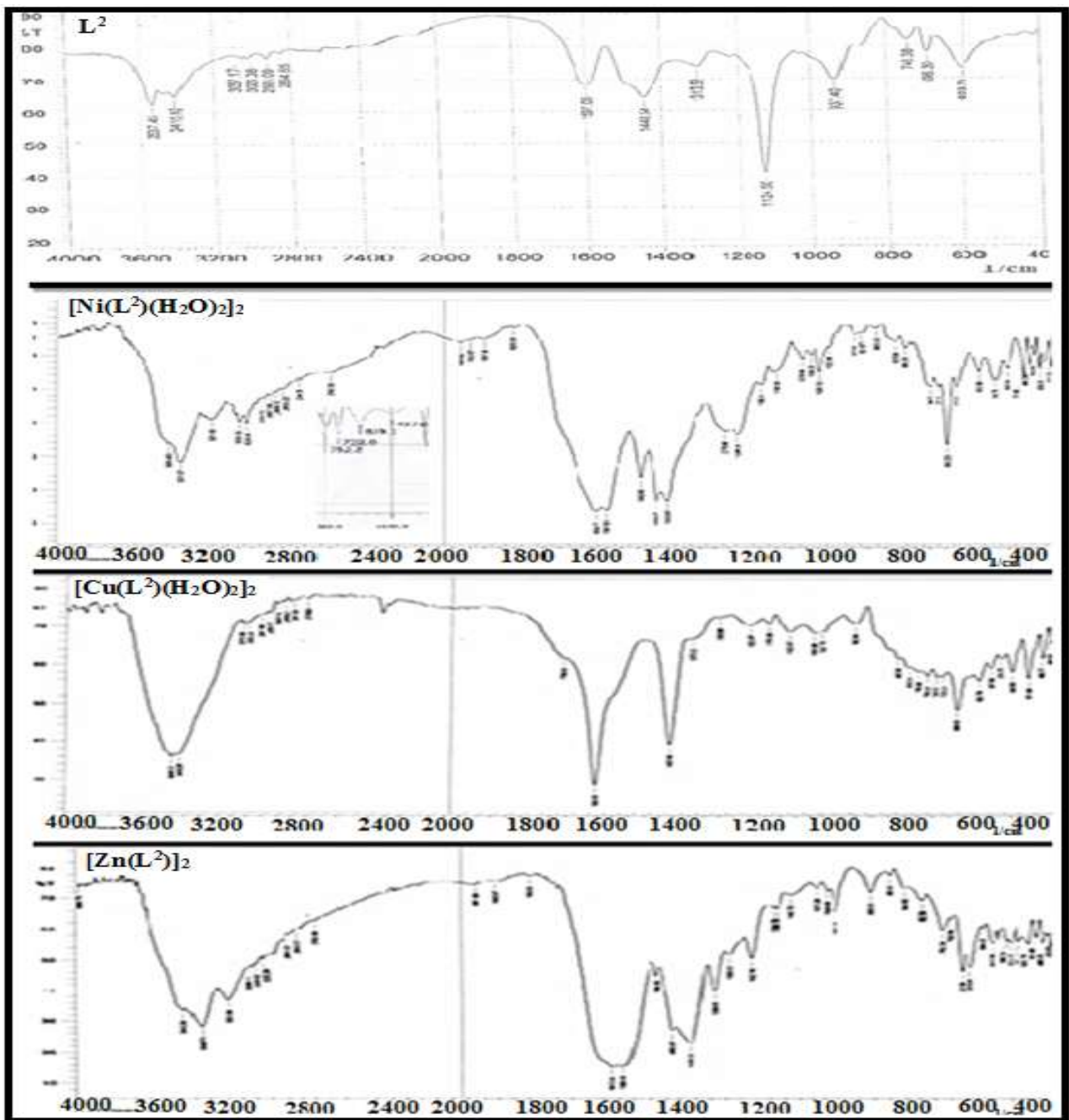


Fig 1-B. FTIR Spectra of L and its complexes with Ni^{II}, Cu^{II} and Zn^{II} metal ions

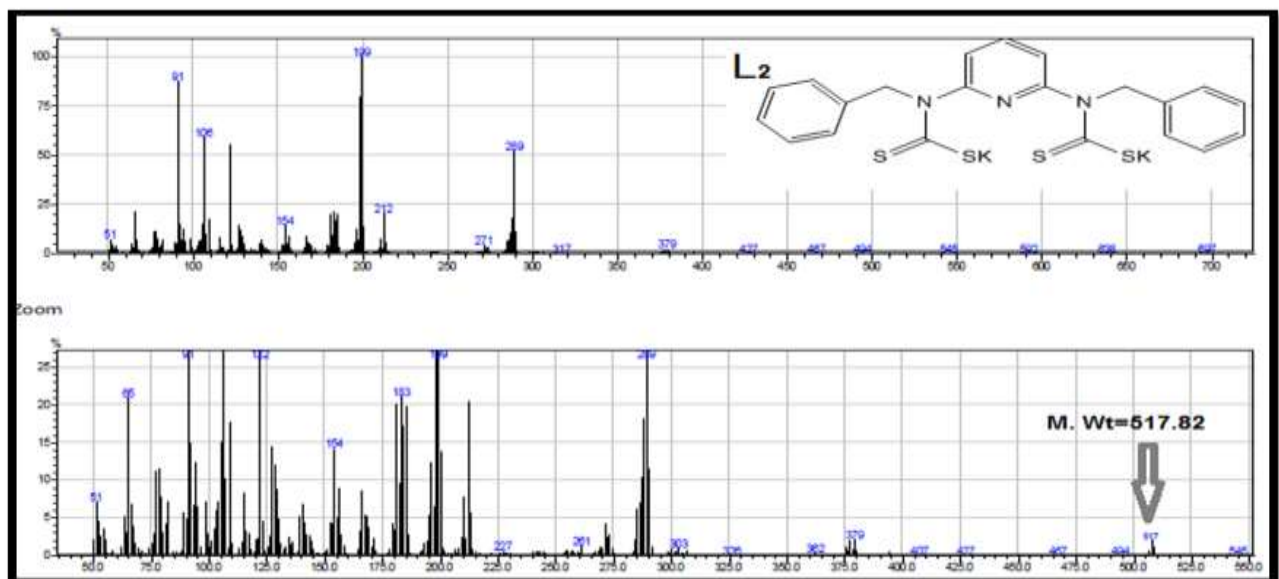


Fig 2: The GC-EI (+) mass spectrum of L

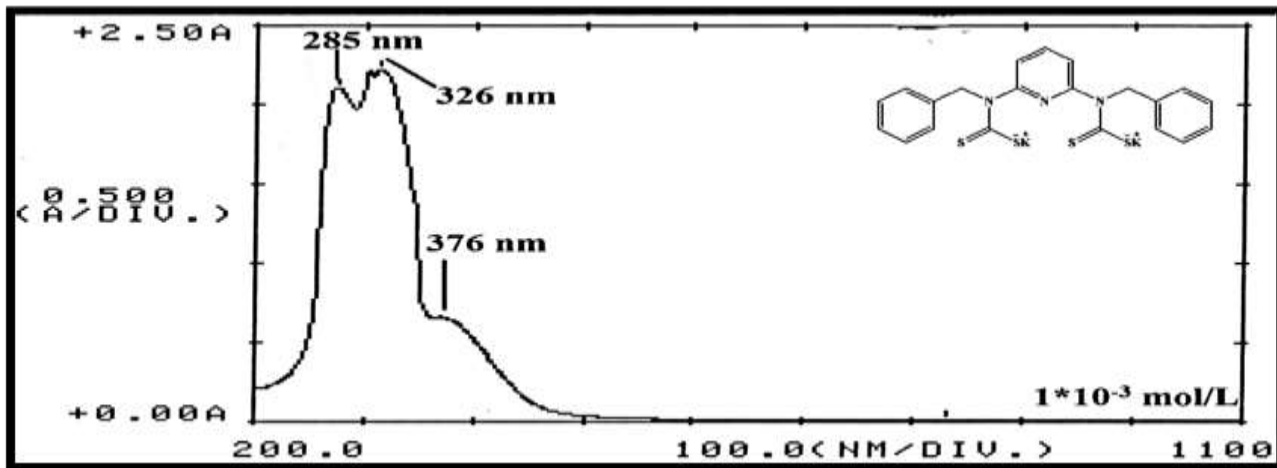


Fig 3: Electronic spectrum of L in DMSO solution

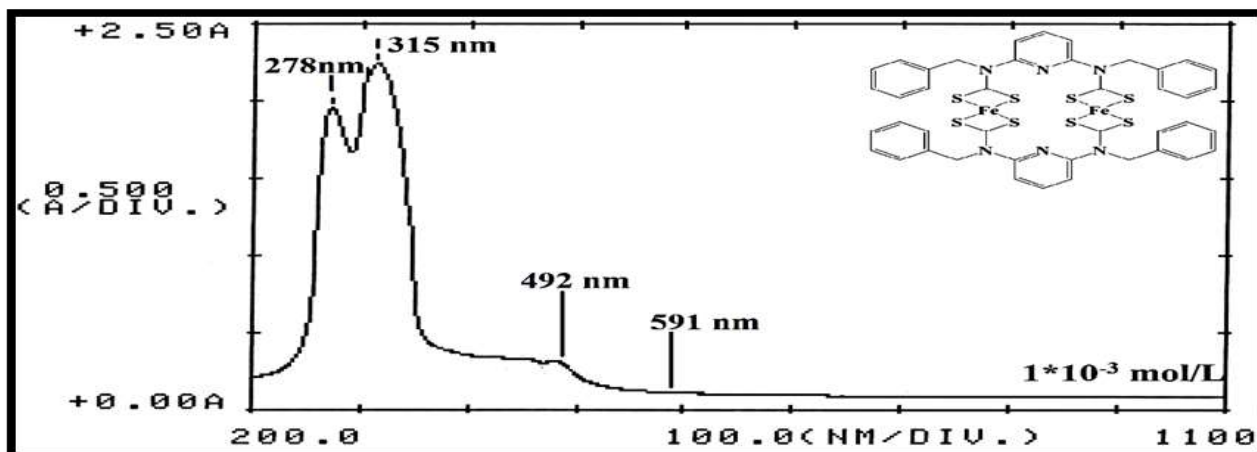


Fig 4: Electronic spectrum of $[Fe(L)]_2$ in DMSO solution

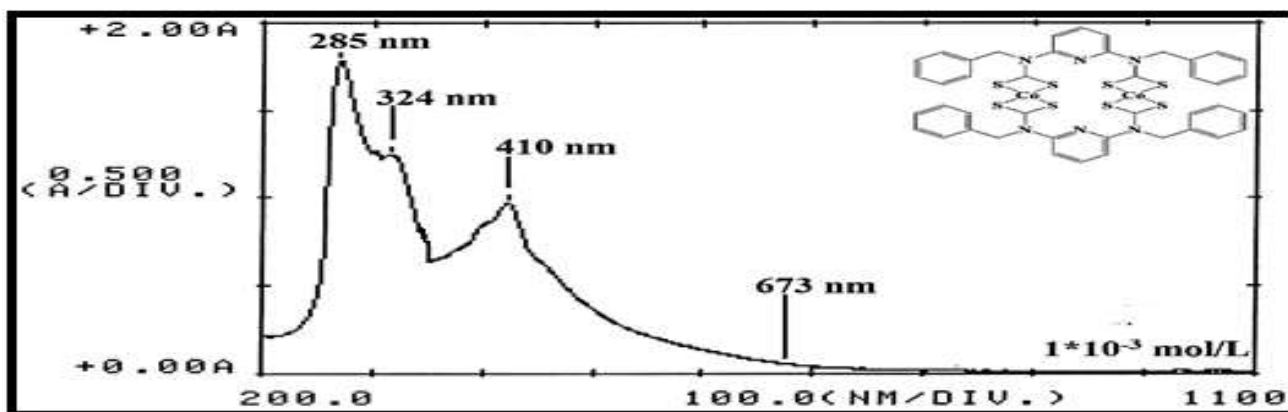


Fig 5: Electronic spectrum of $[Co(L)]_2$ in DMSO solution

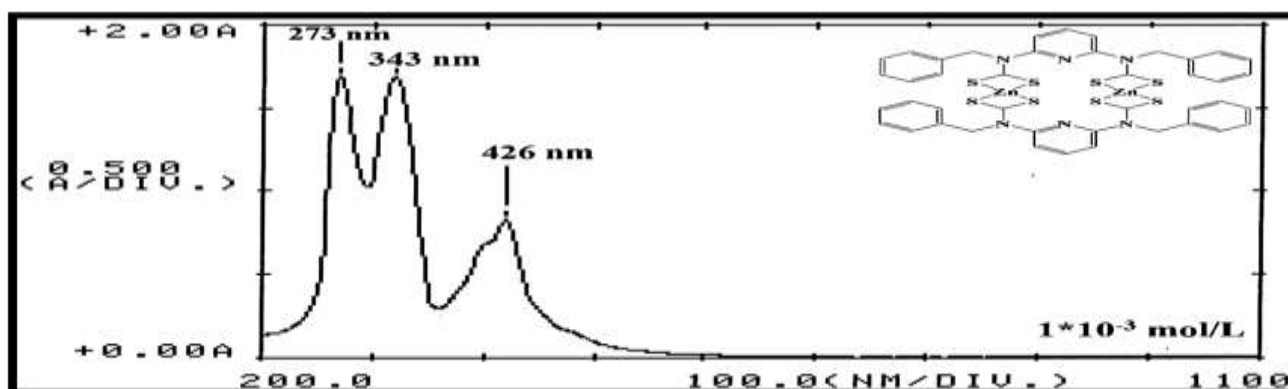


Fig 6: Electronic spectrum of $[Zn(L)]_2$ in DMSO solution

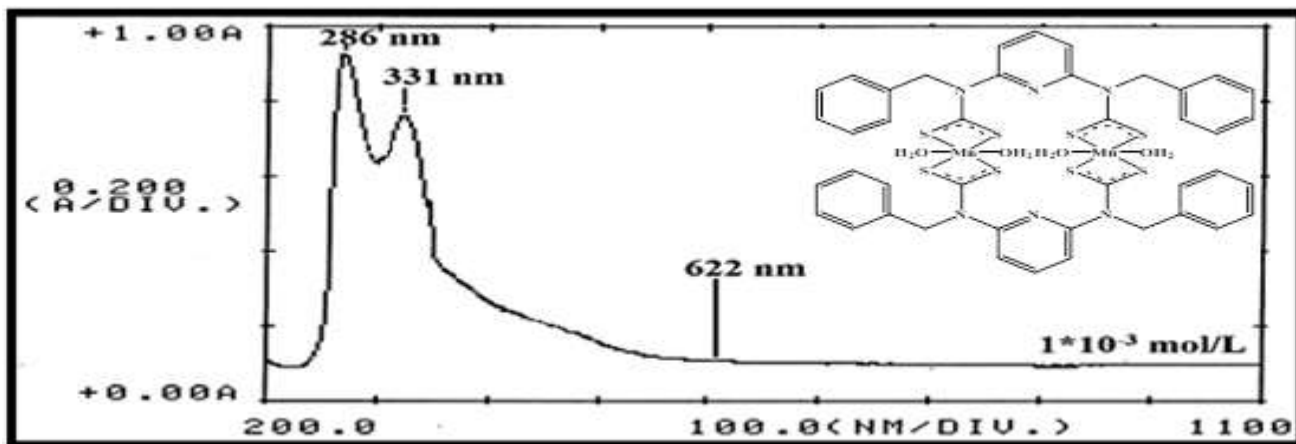


Fig 7: Electronic spectrum of $[Mn(L)(H_2O)_2]_2$ in DMSO solution

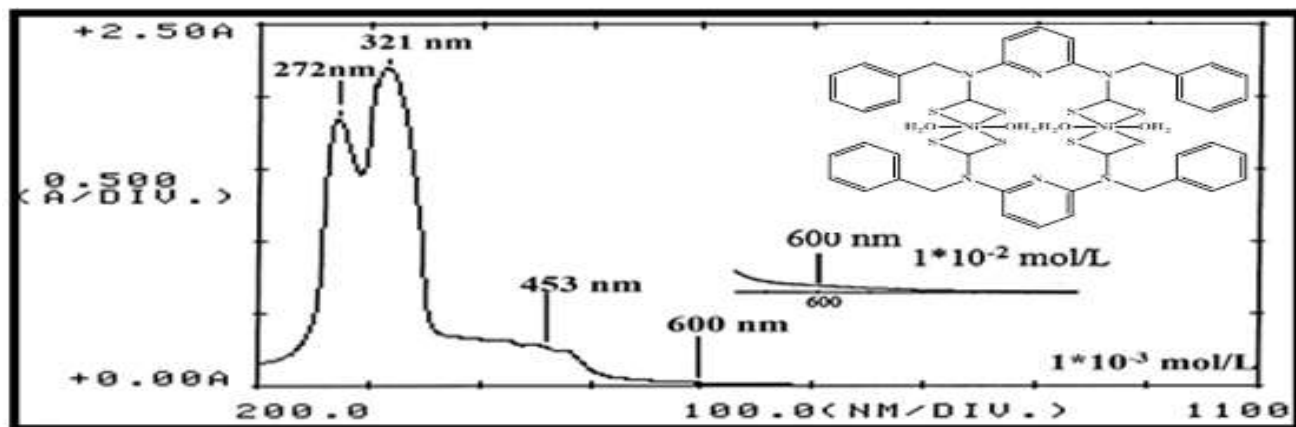


Fig 8: Electronic spectrum of $[Ni(L)(H_2O)_2]_2$ in DMSO solution

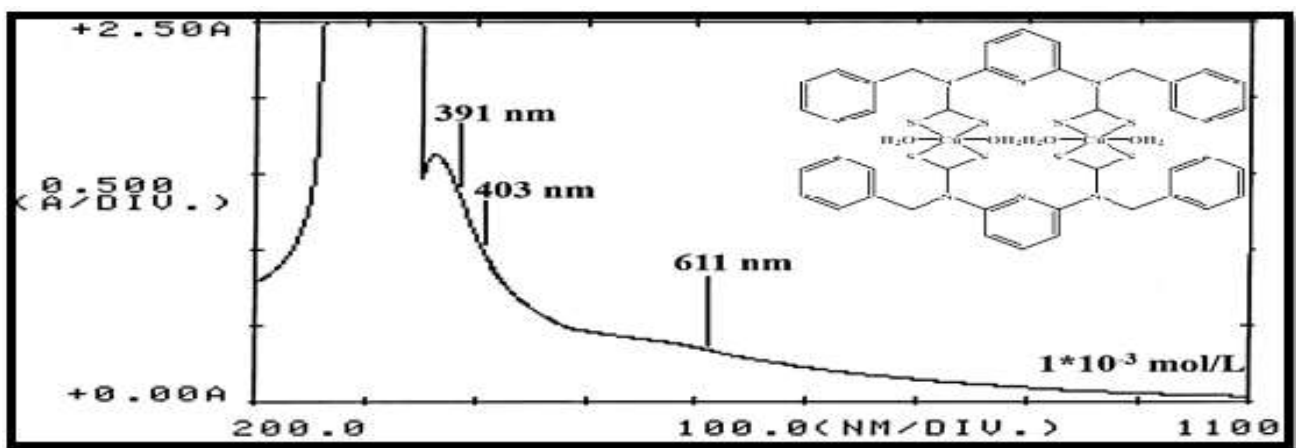


Fig 9: Electronic spectrum of $[Cu(L)(H_2O)_2]_2$ in DMSO solution

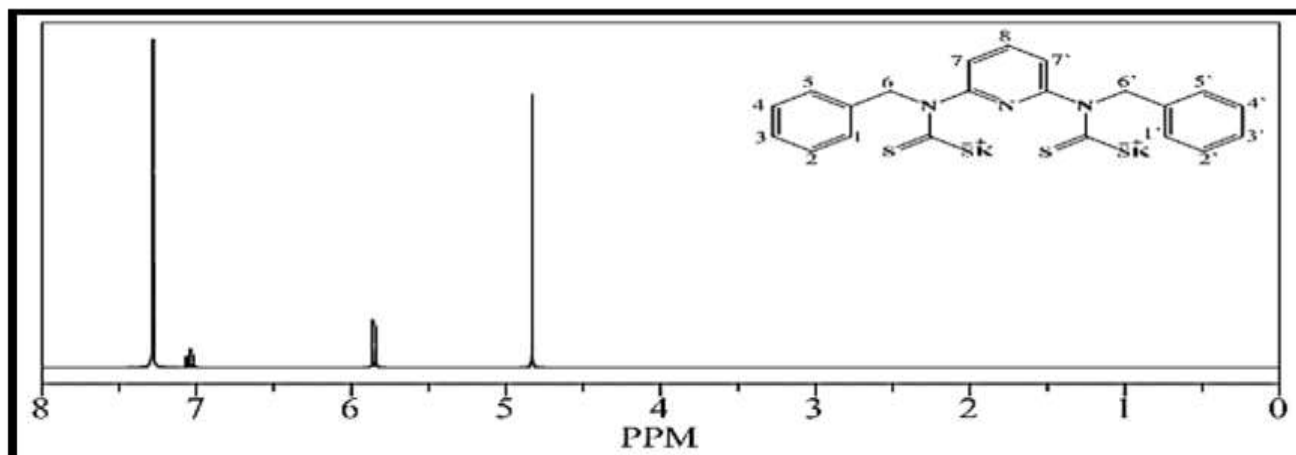


Fig 10: The simulated 1H NMR spectrum of L

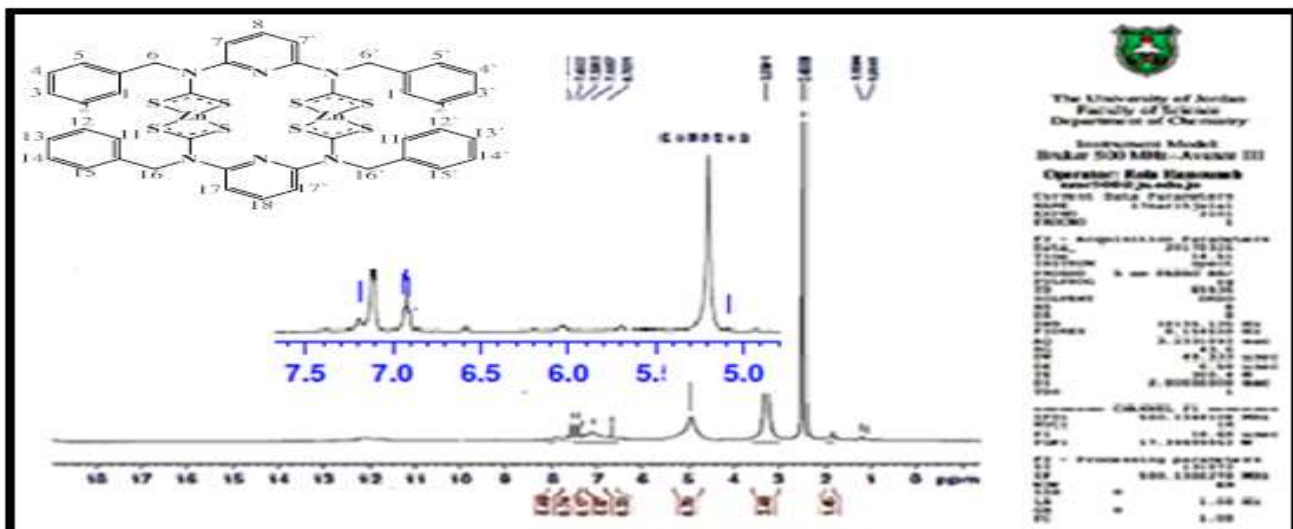
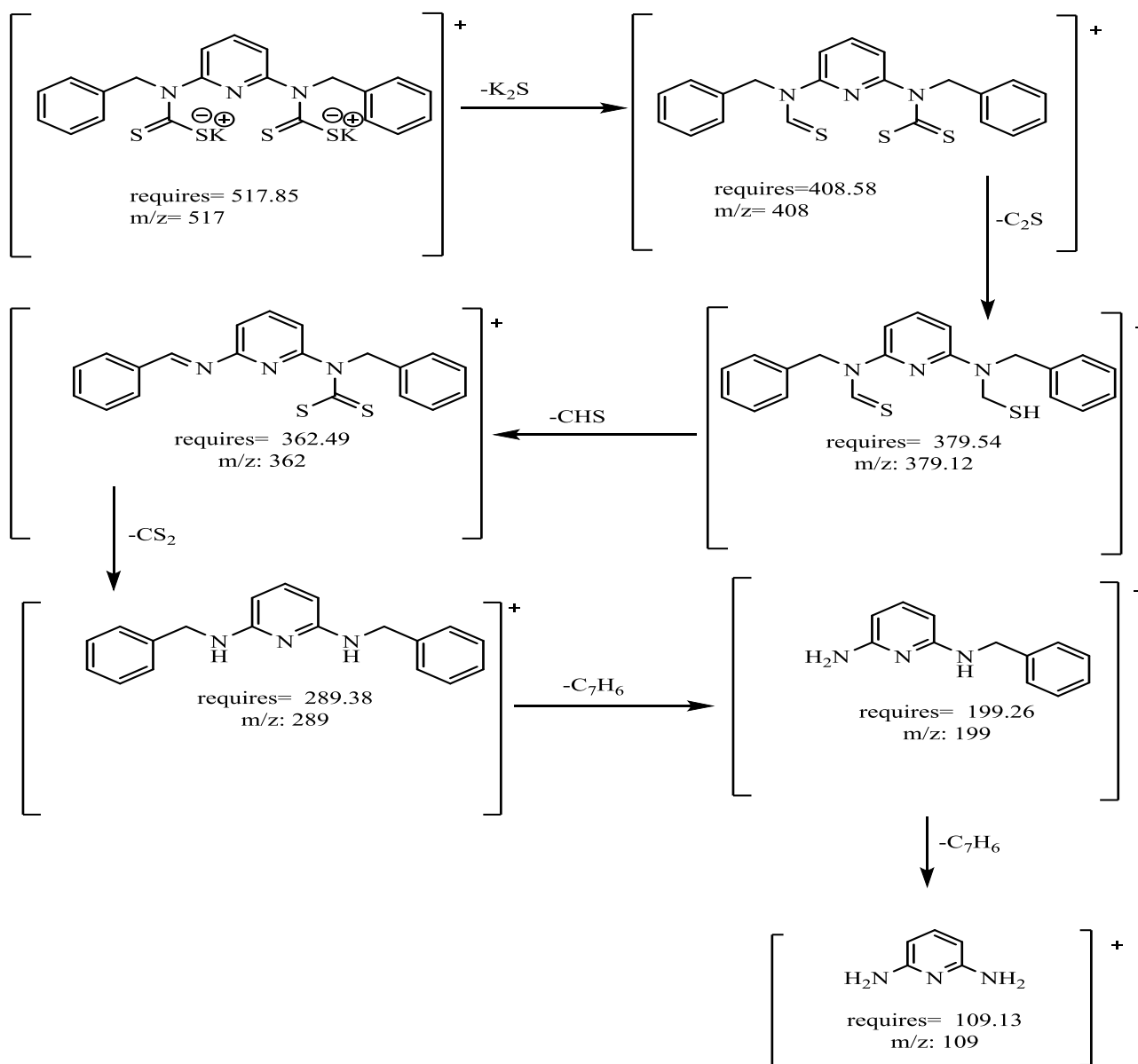


Fig 11: ¹H NMR spectrum of [Zn (L¹)]₂ in DMSO-d₆ solution



Scheme 2: The fragmentation pattern of L